nanomaterials

MDPI

Communication

Preparation of Hydrogen Peroxide Sensitive Nanofilms by a Layer-by-Layer Technique

Kentaro Yoshida [1,*], Tetsuya Ono [1], Takenori Dairaku [1], Yoshitomo Kashiwagi [1] and Katsuhiko Sato [2]

[1] School of Pharmaceutical Sciences, Ohu University 31-1 Misumido, Tomita-machi, Koriyama, Fukushima 963-8611, Japan; t-ono@pha.ohu-u.ac.jp (T.O.); t-dairaku@pha.ohu-u.ac.jp (T.D.); y-kashiwagi@pha.ohu-u.ac.jp (Y.K.)

[2] Graduate School of Pharmaceutical Sciences, Tohoku University, 6-3 Aoba, Aramaki, Aoba-ku, Sendai 980-8578, Japan; satok@m.tohoku.ac.jp

* Correspondence: k-yoshida@pha.ohu-u.ac.jp; Tel.: +81-24-932-8931; Fax: +81-24-933-7372

Received: 24 October 2018; Accepted: 14 November 2018; Published: 15 November 2018

Abstract: H_2O_2-sensitive nanofilms composed of DNA and hemin-appended poly(ethyleneimine) (H-PEI) were prepared by a layer-by-layer deposition of DNA and H-PEI through an electrostatic interaction. The $(H\text{-PEI/DNA})_5$ film was decomposed by addition of 10 mM H_2O_2. H_2O_2-induced decomposition was also confirmed in the hemin-containing $(PEI/DNA)_5$ in which hemin molecules were adsorbed by a noncovalent bond to the nanofilm. On the other hand, the $(PEI/DNA)_5$ film containing no hemin and the $(H\text{-PEI/PSS})_5$ film using PSS instead of DNA did not decompose even with 100 mM H_2O_2. The mechanism of nanofilm decomposition was thought that more reactive oxygen species (ROS) was formed by reaction of hemin and H_2O_2 and then the ROS caused DNA cleavage. As a result $(H\text{-PEI/DNA})_5$ and hemin-containing $(PEI/DNA)_5$ films were decomposed. The decomposition rate of these nanofilms were depended on concentration of H_2O_2, modification ratio of hemin, pH, and ionic strength.

Keywords: hydrogen peroxide response; layer-by-layer; multilayer thin film; nanofilm; stimuli-sensitive

1. Introduction

Functional multilayer thin films have recently been prepared by a layer-by-layer (LbL) deposition technique through electrostatic interaction of polycation and polyanion [1,2]. Synthetic polymers [3,4], proteins [5–7], DNA [8,9], and polysaccharides [10,11] have been used for preparing LbL nanofilms. Such layered thin films have found application in biosensors [5–7], separation and purification [12,13], controlled release of drugs [14–16], and polyelectrolyte microcapsules [17–19]. In addition, stimuli-sensitive LbL films were prepared such as pH [20–22], sugar [23–25], temperature [25], ion [26], and electrical potential-sensitive LbL films [27].

In this work we report the H_2O_2-induced decomposition of LbL nanofilms composed of hemin-appended poly(ethyleneimine) (H-PEI) and DNA. PEI and DNA have positive and negative charge, respectively, and could form LbL multilayer film through electrostatic interaction. Hemin is iron porphyrin molecule and the active cofactor for various enzymes, such as catalase and peroxidase [28]. It is known that the iron porphyrin produces more reactive oxygen species (ROS) such as hydroxy radical (·OH) from reaction with H_2O_2 according to literatures [29,30]. The ROS causes non-specific DNA cleavage [31–34]. Consequently, H-PEI/DNA nanofilm was expected to decompose by addition of H_2O_2 as illustrated in Figure 1. On the other hand, oxidative stress of H_2O_2 related to various diseases caused [35,36]. Therefore, H_2O_2-sensitive gel and nanoparticles were used for the drug delivery system (DDS) [37–40]. It was thought that the H-PEI/DNA nanofilm is also used for DDS for

this purpose by enclosing the drug inside the nanofilm. Actually, $(H\text{-}PEI/DNA)_5$ film was decomposed by addition of H_2O_2 and the decomposition ratio depended on concentration of H_2O_2, modification ratio of hemin, pH, and ionic strength.

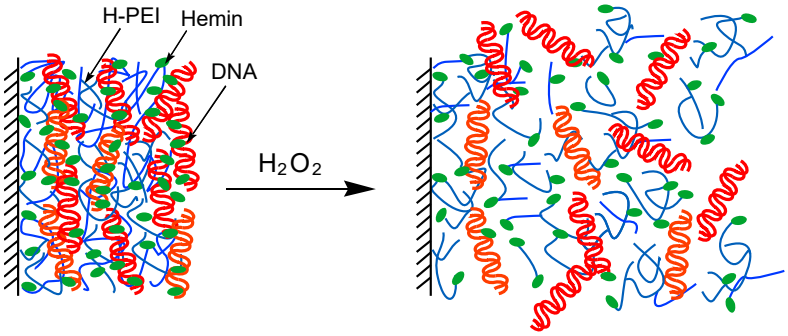

Figure 1. Decomposition of H-PEI/DNA nanofilm by addition of H_2O_2.

2. Materials and Methods

2.1. Materials

Hemin and DNA (calf thymus) were obtained from Sigma-Aldrich Chemical Co. (Wisconsin, WI, USA) and Funakoshi Co. (Kyoto, Japan), respectively. Poly(styrenesulfonate) sodium salt (PSS, molecular weight; 500,000) and poly(allylamine) (PAH, molecular weight; 150,000) were from Scientific Polymer Products, Inc. (Ontario, NY, USA) and Nittobo Co. (Tokyo, Japan). Poly(ethyleneimine) (PEI) was purchased from Nacalai Tesque Inc. (Tokyo, Japan). All other reagents used were of the highest grade and used without further purification.

Hemin-appended PEI (H-PEI) was synthesized as follows. PEI (100 mg) and hemin (37.9 mg) were dissolved in 0.1 M HEPES buffer (pH 7.0), then N-hydroxysuccinimide (8.02 mg) and 1-ethyl-3-(3-dimethylaminopropyl) carbodiimide hydrochloride (13.4 mg) were added in the solution at 4 °C. After 24 h, reaction mixture was purified by dialyzing to water for three days and freeze-dried. The content of hemin residues in PEI was 8.7% (molar ratio of hemin to primary amine), as determined by UV-visible absorption spectroscopy at 390 nm using a molar extinction coefficient of 42,000 M^{-1} cm^{-1} for hemin. Other modification ratio of 1.8%, 4.1%, and 6.5% H-PEI and hemin-appended PAH (H-PAH: modification ratio of 8.0%) were synthesized by similar manners and hemin was added 9.52 mg, 18.98 mg, 28.4 mg and 69.72 mg hemin to 100 mg each polymers, respectively. Chemical structures of hemin, H-PEI, H-PAH, and PSS were shown in Figure 2.

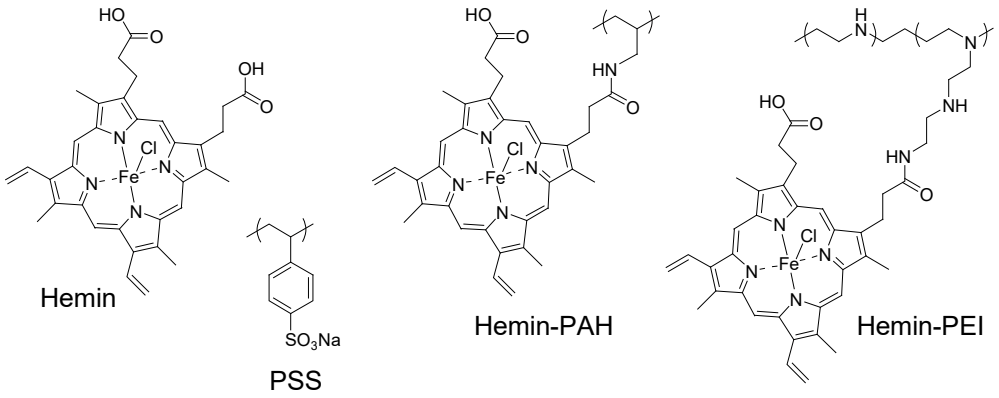

Figure 2. Chemical structures of hemin, H-PAH, H-PEI, and PSS.

2.2. Apparatus

A quartz crystal microbalance (QCM, QCA 917 system, Seiko EG & G, Tokyo, Japan) was used for gravimetric analysis of the LbL films. A 9-MHz AT-cut quartz resonator coated with a thin Au layer (surface area; 0.2 cm^2) was used as a probe, in which the adsorption of 1 ng of substance induces a −0.91 Hz change in the resonance frequency. Atomic force microscope images were recorded on SPM-9600 (SIMADZU). UV–VIS spectrum was recorded on a Shimadzu 3100PC spectrophotometer (Kyoto, Japan).

2.3. Preparation of Nanofilms

H-PEI/DNA nanofilms were prepared on 9 MHz Au-coated quartz resonator for QCM analysis. The quartz resonator was immersed in a H-PEI solution (0.1 mg/mL, in 0.1 M Tris-HCl buffer, pH 7.4) for 15 min to deposit the first H-PEI layer through a hydrophobic force of attraction. After being rinsed in Tris-HCl buffer for 5 min to remove any weakly adsorbed H-PEI, the quartz resonator was immersed in a DNA solution (0.1 mg/mL, in 0.1 M Tris-HCl buffer, pH 7.4) for 15 min to deposit DNA through an electrostatic interaction. The second H-PEI layer was deposited similarly on the surface of the quartz resonator. The deposition was repeated to build up nanofilms. The quartz slide was cleaned by chromic acid mixture before use. $(PEI/DNA)_5$, $(H\text{-}PAH/DNA)_5$ and $(H\text{-}PEI/PSS)_5$ nanofilms were prepared by a same manner. Hemin-containing $(PEI/DNA)_5$ and $(PAH/DNA)_5$ films were prepared by immersing $(PEI/DNA)_5$ and $(PAH/PSS)_5$ films in 0.1 mg/mL hemin solutions into 15 min, respectively, followed by immersing 0.1 M Tris-HCl buffer for 5 min to remove any weakly adsorbed hemin.

2.4. Decomposition of Nanofilms

The H_2O_2-induced decomposition of the nanofilms was studied by monitoring the resonance frequency change (ΔF) of the 5-bilayer film-coated quartz resonator in a flow-through cell of QCM. The H_2O_2 solution was injected to the flow-through cell to monitor the decomposition of the nanofilm and the decomposition characteristic was evaluated by ΔF after 1 h. All experiments were carried out at room temperature (ca. 20 °C).

2.5. Observation of Nanofilms with AFM

For AFM observation, $(H\text{-}PEI/DNA)_5$ nanofilm was prepared on a circular glass slide (diameter was 1.5 cm) which was cleaned using fuming nitric acid and thoroughly rinsed in distilled water. The glass slide was immersed in distilled water two times of 30 min to desalt and dried in a desiccator for three days. Then the film was cut with an ultrasonic cutter (USW-333, Honda Electronics Co., LTD., Aichi, Japan) and the surface and thickness of the film were observed. In addition, the $(H\text{-}PEI/DNA)_5$ nanofilm was immersed in 100 mM of H_2O_2 solution one hour to disintegrate and observed by a similar manner. All AFM images were taken in contact mode using Olympus microcantilevers (OMCL-TR800PSA-1, Olympus Co., Tokyo, Japan) at room temperature in air.

3. Results and Discussion

Figure 3 shows the change in the resonance frequency (ΔF) of a QCM observed on depositing H-PEI and DNA on the quartz resonator. The ΔF values decreased on deposition of both H-PEI and DNA, showing that H-PEI and DNA could form a LbL nanofilm. It is reasonable that H-PEI and DNA form the H-PEI/DNA film, because PEI and DNA could bind through the electrostatic interaction (PEI and DNA are polycation and polyanicon, respectively). Deposition amount of H-PEI and DNA were 1.33 μg/cm^2 and 12.8 μg/cm^2 in $(H\text{-}PEI/DNA)_5$ film. Hemin was appended to PEI at 8.7% for primary amin of PEI (PEI contains primary, secondary, and tertiary amines at 1:2:1 [41]). It was estimated that $(H\text{-}PEI/DNA)_5$ film contained 6.17 μmol/cm^2 of hemin molecules.

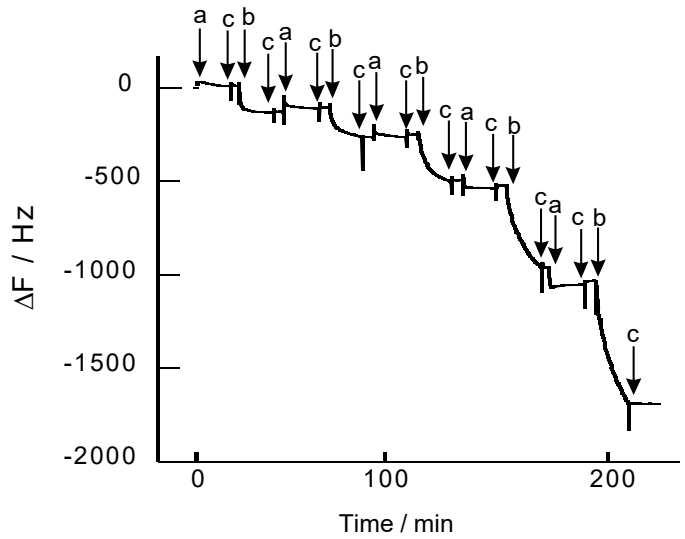

Figure 3. Typical QCM response for the deposition of LbL films constructed of H-PEI and DNA at pH 7.4. The quartz resonator was exposed to 0.1 mg/mL H-PEI (modification ratio of 8.7%) (**a**), 0.1 mg/mL DNA (**b**), and 0.1 M Tris-HCl buffer solution (**c**).

The H_2O_2-induced decomposition of a $(H\text{-}PEI/DNA)_5$ film was investigated on QCM (Figure 4). ΔF has not changed in buffer solution, suggesting the $(H\text{-}PEI/DNA)_5$ film was stable in this condition. By contrast, the ΔF increased when a 100 mM H_2O_2 solution was applied. In the case of exposing $(H\text{-}PEI/DNA)_5$ film to 100 mM H_2O_2, ΔF was increase 1500 Hz after 1 h, and it showed that ca. 90% weight of $(H\text{-}PEI/DNA)_5$ film exfoliated from the quartz slide. The increase of ΔF depended on concentration of H_2O_2. When $(H\text{-}PEI/DNA)_5$ films were exposed to 10, 20, 50, and 100 mM H_2O_2 solutions, these decomposition ratios were 18.7, 22.0, 44.2, and 95.1%, respectively.

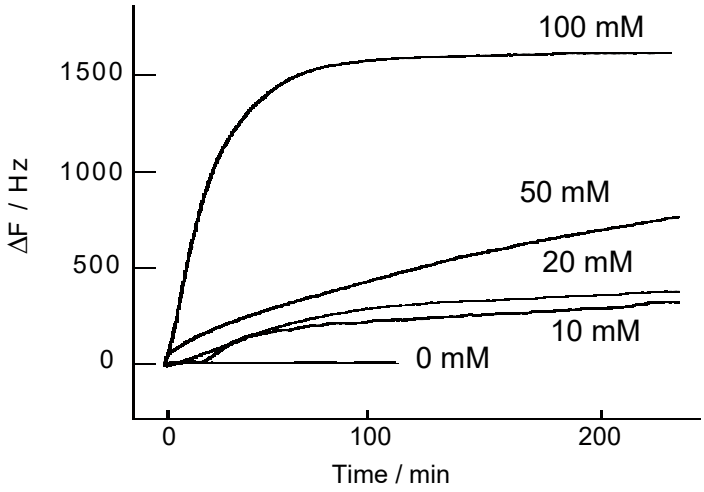

Figure 4. QCM frequence change of the $(H\text{-}PEI/DNA)_5$ films in the presence of H_2O_2 in 0.1 M Tris-HCl buffer solution (pH 7.0).

The surface morphology and thickness of $(H\text{-}PEI/DNA)_5$ film was observed by AFM (Figure 5). The surface of $(H\text{-}PEI/DNA)_5$ film was rough and average thickness was estimated at 27.7 nm from cross section (Figure 5a). On the other hand, the surface of $(H\text{-}PEI/DNA)_5$ film was smooth and average thickness was decreased at 2.7 nm after exposure to H_2O_2 (Figure 5b). The thickness of $(H\text{-}PEI/DNA)_5$ film was decreased by H_2O_2 processing. It was suggested that $(H\text{-}PEI/DNA)_5$ film was decomposed by H_2O_2.

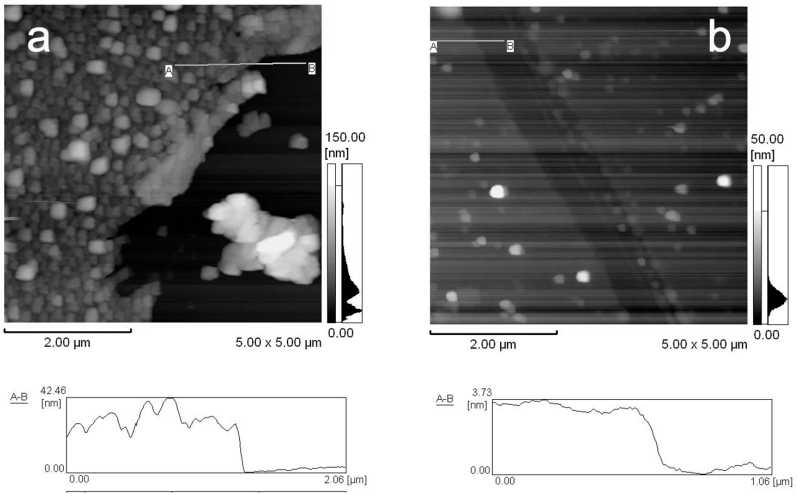

Figure 5. AFM images of $(H\text{-}PEI/DNA)_5$ film (**a**) and after exposure to 100 mM H_2O_2 (**b**).

To investigate the mechanism of the $(H\text{-}PEI/DNA)_5$ film decomposition, various polymers were used for H_2O_2-sensitive LBL film preparation and these films were tested (Figure 6). $(H\text{-}PEH/DNA)_5$ film was decomposed at 96% by addition of 100 mM H_2O_2 solution after 1 h. By contrast, the decomposition rate of $(PEI/DNA)_5$ which did not contain hemin molecules was 3.6%. A hemin-containing $(PEI/DNA)_5$ film in which hemin was adsorbed by a noncovalent bond after preparation of film was decomposed 85.5% by H_2O_2. These results suggested that hemin molecules were necessary for H_2O_2 decomposition of nanofilms for producing of ROS from reaction with H_2O_2. The decomposition rate of the $(H\text{-}PEI/PSS)_5$ film prepared using PSS instead of DNA and $(H\text{-}PAH/DNA)_5$ film prepared using PAH instead of PEI were 2.6% and 8.4% under same conditions. It was thought that LbL nanofilms composed of PEI and DNA were convenient for H_2O_2 response. The ROS effectively cleaved DNA more than PSS. In addition, PEI was branched polycation and its electric charge density is lower than that of liner polycation of PAH. Low charge density of PEI was useful for degradation. Porphyrin molecules such as hemin could interact with a major groove of DNA [42,43]. It was known that PEI binding porphyrin could interact with DNA effectively than PAH binding one [43]. Therefore, $(H\text{-}PEH/DNA)_5$ and hemin-containing $(PEI/DNA)_5$ film were decomposed by H_2O_2 more effectively than other nanofilms.

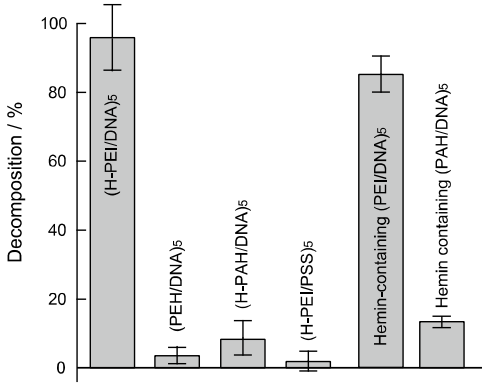

Figure 6. Decomposition ratio of $(H\text{-}PEI/DNA)_5$, $(PEI/DNA)_5$, $(H\text{-}PAH/DNA)_5$, $(H\text{-}PEI/PSS)_5$, hemin-containing $(PEI/DNA)_5$ and hemin-containing $(PAH/DNA)_5$ films after immersed in 100 mM H_2O_2 (0.1 M Tris-HCl buffer solution (pH 7.0) after 1 h. Modification ratio of H-PEI and H-PAH were 8.7% and 8.0%, respectively. Hemin-containing $(PEI/DNA)_5$ and hemin-containing $(PAH/DNA)_5$ films was prepared by immersed $(PEI/DNA)_5$ and $(PAH/DNA)_5$ films in 0.1 mg/mL hemin solution. Error bars represent standard deviation (n = 4).

The decomposition properties of $(H\text{-}PEI/DNA)_5$ film were investigated under various conditions. Figure 7A shows the effect of hemin modification ratio in PEI on decomposition ratio of $(H\text{-}PEI/DNA)_5$ films. The $(H\text{-}PEI/DNA)_5$ film which used modification ratio of 6.5% and 4.1% H-PEI film were more sensitive than 1.8% of one, because these films could react effectively with H_2O_2 by lot of hemin molecules in film. However, decomposition of modification ratio of 8.7% hemin film was decreased. We thought that the interaction between hemin and DNA was excessively formed in nanofilm and disturbed the decomposition of the film. Effects of reaction solution pH and ion strength were studied (Figure 7B,C). The pH 9 solution decomposed $(H\text{-}PEI/DNA)_5$ film effectively more than pH 4 and pH 7 solutions. The interaction for $(H\text{-}PEI/DNA)_5$ film formation weakened, because positive charge of PEI was decreased in pH 9 solution. Thus, H-PEI and DNA interaction for composition of LbL film was decreased and LbL film was decomposed low concentration of H_2O_2. Similarly, high ion strength reduced electrostatic interaction of PEI and DNA for LbL film. Therefore, $(H\text{-}PEI/DAN)_5$ film was decomposed by low concentration of H_2O_2 in 300 mM NaCl solution (Figure 7C).

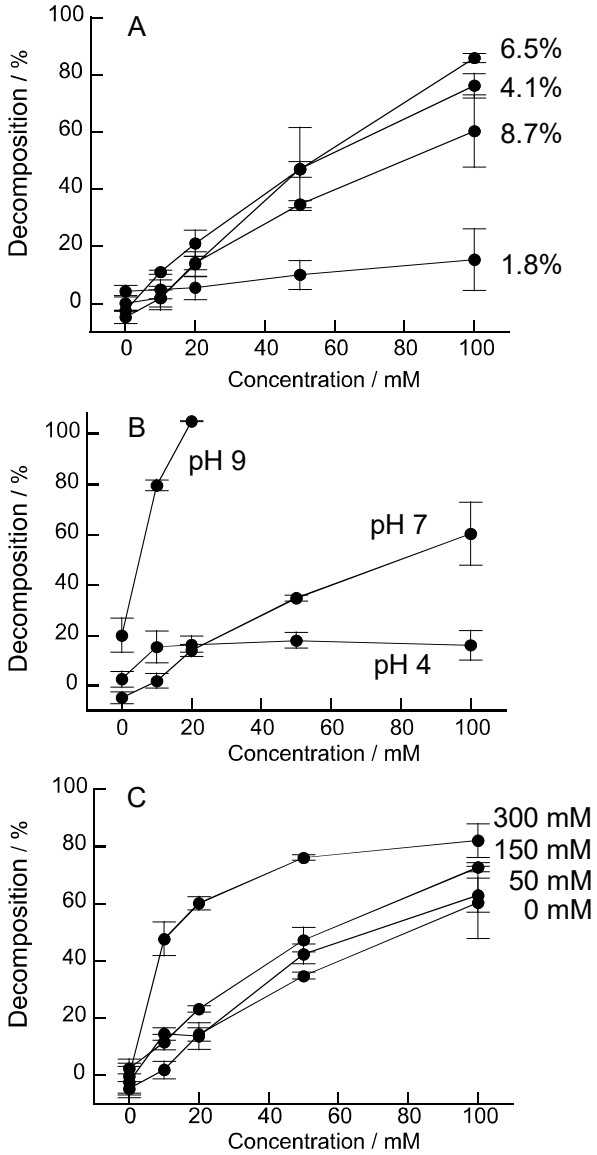

Figure 7. Effect of modification ratio of hemin (**A**), pH (**B**), and ion strength (**C**) on the H_2O_2-induced decomposition properties of $(H\text{-}PEI/DNA)_5$ film. H-PEI of (**B**,**C**) were 8.7% modification ratio. Error bars represent standard deviation (n = 4).

The decomposition properties of hemin-containing $(PEI/DNA)_5$ films were investigated similarly. Figure 8A shows the decomposition ratio of hemin-containing $(PEI/DNA)_5$ films prepared by immersing in 0.1 mg/mL and 0.01 mg/mL hemin solutions to absorb on nanofilm and these films contained 2.27 nmol/cm^2 and 1.09 nmol/cm^2 hemin molecules, respectively. The decomposition ratio of hemin-containing $(PEI/DNA)_5$ film increased with increasing hemin content in film. However, hemin-containing $(PEI/DNA)_5$ film (1.0 mg/mL) and $(H\text{-}PEI/DNA)_5$ (6.5%) film were 62% and 85%, respectively. It seems that introduce hemin molecules into the LbL film by covalent bond was effective for the decomposition of the LbL film. Effects of reaction solution pH and ion strength were studied (Figure 8B,C). The pH 9 solution decomposed hemin-containing $(PEI/DNA)_5$ films film effectively more than pH 4 and pH 7 solutions from same reason of $(H\text{-}PEI/DNA)_5$ film. However, the ionic strength did not effect on the collapse of the film. When hemin molecules adsorbed into $(PEI/DNA)_5$ film, counter ions were also adsorbed. The effect of the ion strength of the reaction solution was reduced.

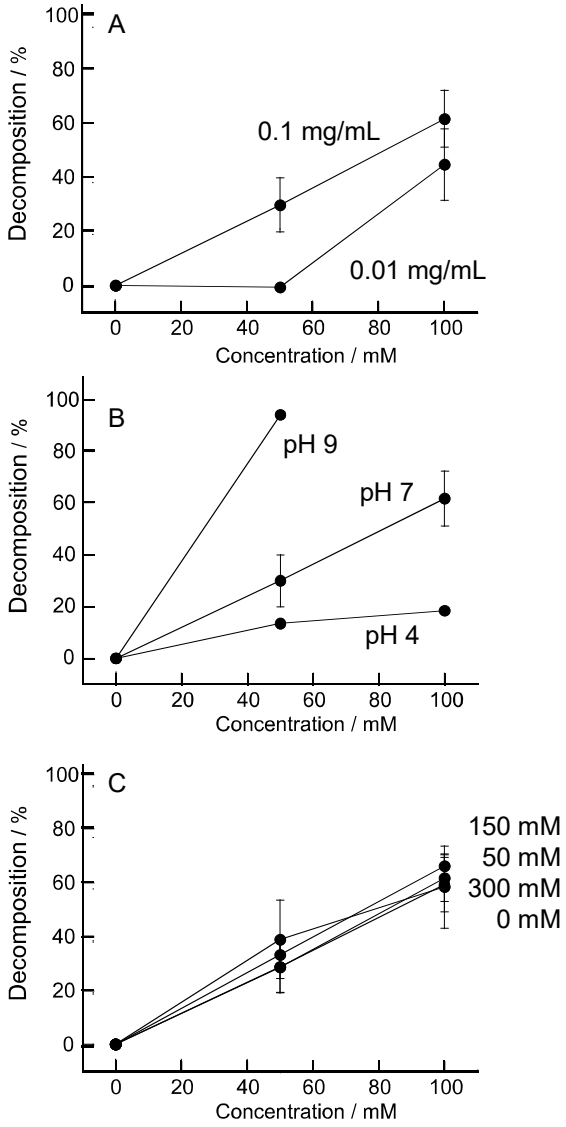

Figure 8. Effect of concentration of hemin solution to adsorb (**A**), pH (**B**), and ion strength (**C**) on the H_2O_2-induced decomposition properties of hemin-containing $(PEI/DNA)_5$. Hemin-containing $(PEI/DNA)_5$ of (**B**,**C**) were prepared by 0.1 mg/mL hemin solution. Error bars represent standard deviation (n = 4).

4. Conclusions

The $(H\text{-}PEI/DNA)_5$ and hemin-containing $(PEI/DNA)_5$ nanofilms were prepared by LbL technique and were decomposed by addition of H_2O_2. The decomposition depended on modification rate of hemin, concentration of H_2O_2, pH and ion strength of reaction solution. We have previously reported H_2O_2 sensitive nanofilms using the reaction of phenylboronic acid to phenol by H_2O_2 [44,45]. We also developed glucose and lactate stimuli responsive nanofilm combining this thin film with the enzymatic reaction of glucose oxidase [46] and lactate oxidase [47] (These enzymes produce H_2O_2 from each substrate). These nanofilms responded to each stimulus and decomposed within several minutes under physiological conditions, suggesting the application of insulin and anticancer drugs to DDS. However, there are some drugs that sustained release is desirable for DDS applications. The $(H\text{-}PEI/DNA)_5$ and hemin-containing $(PEI/DNA)_5$ nanofilms showed sustained degradation against low concentration H_2O_2. If the carrier containing drugs can be degraded persistently, it may be achieved as sustained drug release carrier by using this hemin base nanofilm.

Author Contributions: K.S. designed the work. K.Y., Y.K., and K.S. collected the materials. K.Y., T.D., T.O., and K.S. were involved in the experimental works. The manuscript was prepared by K.Y. and K.S.

Funding: This work was supported JSPS KAKENHI grants (numbers JP16K08189, JP18K06791, and JP18K19936).

Acknowledgments: This work was partially supported by JSPS KAKENHI grants (numbers JP16K08189, JP18K06791, and JP18K19936).

Conflicts of Interest: The authors declare no conflicts of interest.

References

1. Decher, G.; Hong, J.D. Buildup of ultrathin multilayer films by a self-assembly process, 1 consecutive adsorption of anionic and cationic bipolar amphiphiles on charged surfaces. *Makromol. Chem. Macromol. Symp.* **1991**, *46*, 321–327. [CrossRef]
2. Decher, G. Fuzzy Nanoassemblies: Toward layered polymeric multicomposites. *Science* **1997**, *277*, 1232–1237. [CrossRef]
3. He, T.; Jańczewski, D.; Guo, S.; Man, S.M.; Jiang, S.; Tan, W.S. Stable pH responsive layer-by-layer assemblies of partially hydrolysed poly(2-ethyl-2-oxazoline) and poly(acrylic acid) for effective prevention of protein, cell and bacteria surface attachment. *Colloids Surf. B Biointerfaces* **2018**, *161*, 269–278. [CrossRef] [PubMed]
4. Bellanger, H.; Casdorff, K.; Muff, L.F.; Ammann, R.; Burgert, I.; Michen, B. Layer-by-layer deposition on a heterogeneous surface: Effect of sorption kinetics on the growth of polyelectrolyte multilayers. *J. Colloid Interface Sci.* **2017**, *500*, 133–141. [CrossRef] [PubMed]
5. Zhao, W.; Xu, J.J.; Chen, H.Y. Electrochemical biosensors based on layer-by-layer assemblies. *Electroanalysis* **2006**, *18*, 1737–1748. [CrossRef]
6. Hoshi, T.; Anzai, J.; Osa, T. Controlled deposition of glucose oxidase on platinum electrode based on an avidin/biotin system for the regulation of output current of glucose sensors. *Anal. Chem.* **1995**, *67*, 770–774. [CrossRef] [PubMed]
7. Dai, Z.; Wilson, J.T.; Chaikof, E.L. Construction of pegylated multilayer architectures via (strept)avidin/biotin interactions. *Mater. Sci. Eng. C* **2007**, *27*, 402–408. [CrossRef]
8. Zelikin, A.N.; Becker, A.L.; Johnston, A.P.R.; Wark, K.L.; Turatti, F.; Caruso, F. A general approach for DNA encapsulation in degradable polymer microcapsules. *ACS Nano* **2007**, *1*, 63–69. [CrossRef] [PubMed]
9. Shchukin, D.G.; Patel, A.A.; Sukhorukov, G.B.; Lvov, Y.M. Nanoassembly of biodegradable microcapsules for DNA encasing. *J. Am. Chem. Soc.* **2004**, *126*, 3374–3375. [CrossRef] [PubMed]
10. Itoh, Y.; Matsusaki, M.; Kida, T.; Akashi, M. Enzyme-responsive release of encapsulated proteins from biodegradable hollow capsules. *Biomacromolecules* **2006**, *7*, 2715–2718. [CrossRef] [PubMed]
11. Chinnayelka, S.; McShane, M.J. Glucose-sensitive nanoassemblies comprising affinity-binding complexes trapped in fuzzy microshells. *J. Fluoresc.* **2004**, *14*, 585–595. [CrossRef] [PubMed]
12. Hoffman, K.; Tieke, B. Layer-by-layer assembled membranes containing hexacyclen-hexaacetic acid and polyethyleneimine N-acetic acid and their ion selective permeation behavior. *J. Membr. Sci.* **2009**, *341*, 261–267. [CrossRef]

13. Huang, Z.; Li, M.; Li, N.; Tang, X.; Ouyang, Z. Antibacterial properties enhancement of layer-by-layer self-assembled nanofiltration membranes. *J. Nanosci. Nanotechnol.* **2018**, *18*, 4524–4533. [CrossRef] [PubMed]
14. Sato, K.; Yoshida, K.; Takahashi, S.; Anzai, J. pH- and sugar-sensitive layer-by-layer films and microcapsules for drug delivery. *Adv. Drug Deliv. Rev.* **2011**, *63*, 809–821. [CrossRef] [PubMed]
15. Choi, D.; Hong, J. Layer-by-layer assembly of multilayer films for controlled drug release. *Arch. Pharm. Res.* **2014**, *37*, 79–87. [CrossRef] [PubMed]
16. Nolan, C.M.; Serpe, M.J.; Lyon, L.A. Thermally modulated insulin release from microgel thin films. *Biomacromolecules* **2004**, *5*, 1940–1946. [CrossRef] [PubMed]
17. Donath, E.; Sukhorukov, G.B.; Caruso, F.; Davis, S.A.; Möhwald, H. Novel hollow polymer shells by colloid-templated assembly of polyelectrolytes. *Angew. Chem. Int. Ed.* **1998**, *37*, 2201–2205. [CrossRef]
18. Mercato, L.L.D.; Ferraro, M.M.; Baldassarre, F.; Mancarella, S.; Greco, V.; Rinaldi, R.; Leporatti, S. Biological applications of LbL multilayer capsules: From drug delivery to sensing. *Adv. Colloid Interface Sci.* **2014**, *207*, 139–154. [CrossRef] [PubMed]
19. Tong, W.; Song, X.; Gao, C. Layer-by-layer assembly of microcapsules and their biomedical applications. *Chem. Soc. Rev.* **2012**, *41*, 6103–6124. [CrossRef] [PubMed]
20. Biesheuvel, P.M.; Mauser, T.; Sukhorukov, G.B.; Möhwald, H. Micromechanical theory for pH-dependent polyelectrolyte multilayer capsule swelling. *Macromolecules* **2006**, *39*, 8480–8486. [CrossRef]
21. Kozlovskaya, V.; Sukhishvili, S.A. Amphoteric hydrogel capsules: Multiple encapsulation and release routes. *Macromolecules* **2006**, *39*, 6191–6199. [CrossRef]
22. Levy, T.; De'jugnat, C.; Sukhorukov, G.B. Polymer microcapsules with carbohydrate-sensitive properties. *Adv. Funct. Mater.* **2008**, *18*, 1586–1594. [CrossRef]
23. Geest, B.G.D.; Jonas, A.M.; Demeester, J.; Smedt, S.C.D. Glucose-responsive polyelectrolyte capsules. *Langmuir* **2006**, *22*, 5070–5074. [CrossRef] [PubMed]
24. Chinnayelka, S.; McShane, M.J. Microcapsule biosensors using competitive binding resonance energy transfer assays based on apoenzymes. *Anal. Chem.* **2005**, *77*, 5501–5511. [CrossRef] [PubMed]
25. Prevot, M.; Déjugnat, C.; Mçhwald, H.; Sukhorukov, G.B. Behavior of temperature-sensitive PNIPAM confined in polyelectrolyte capsules. *Chem. Phys. Chem.* **2006**, *7*, 2497–2502. [CrossRef] [PubMed]
26. Selin, V.; Ankner, J.F.; Sukhishvili, S.A. Diffusional response of layer-by-layer assembled polyelectrolyte chains to salt annealing. *Macromolecules* **2015**, *48*, 3983–3990. [CrossRef]
27. Schmidt, D.J.; Moskowitz, J.S.; Hammond, P.T. Electrically triggered release of a small molecule drug from a polyelectrolyte multilayer coating. *Chem. Mater.* **2010**, *22*, 6416–6425. [CrossRef] [PubMed]
28. Travascio, P.; Li, Y.S.D. DNA-enhanced peroxidase activity of a DNA-aptamer-hemin complex. *Chem. Biol.* **1998**, *5*, 505–517. [CrossRef]
29. Yao, Y.; Mao, Y.; Huang, Q.; Wang, L.; Huang, Z.; Lu, W.; Chen, W. Enhanced decomposition of dyes by hemin-ACF with significant improvement in pH tolerance and stability. *J. Hazard. Mater.* **2014**, *264*, 323–331. [CrossRef] [PubMed]
30. Jiang, B.; Yao, Y.; Xie, R.; Dai, D.; Lu, W.; Chen, W.; Zang, L. Enhanced generation of reactive oxygen species for efficient pollutant elimination catalyzed by hemin based on persistent free radicals. *Appl. Catal. B Environ.* **2016**, *183*, 291–297. [CrossRef]
31. Breen, A.P.; Murphy, J.A. Reactions of oxyl radicals with DNA. *Free Radic. Biol. Med.* **1995**, *18*, 1033–1077. [CrossRef]
32. Hertzberg, R.P.; Dervan, P.B. Cleavage of DNA with methidiumpropyl-EDTA-iron(II): Reaction conditions and product analyses. *Biochemistry* **1984**, *23*, 3934–3945. [CrossRef] [PubMed]
33. Sigman, D.S. Nuclease activity of 1,10-phenanthroline-copper ion. *Acc. Chem. Res.* **1986**, *19*, 180–186. [CrossRef]
34. Kawanishi, S.; Oikawa, S.; Murata, M.; Tsukitome, H.; Saito, I. Site-specific oxidation at GG and GGG sequences in double-stranded DNA by benzoyl peroxide as a tumor promoter. *Biochemistry* **1999**, *51*, 16733–16739. [CrossRef]
35. Drechsel, D.A.; Patel, M. Role of reactive oxygen species in the neurotoxicity of environmental agents implicated in Parkinson's disease. *Free Radic. Biol. Med.* **2008**, *44*, 1873–1886. [CrossRef] [PubMed]
36. Liou, G.Y.; Storz, P. Reactive oxygen species in cancer. *Free Radic. Res.* **2010**, *44*, 479–496. [CrossRef] [PubMed]

37. De Gracia, L.C.; Joshi-Barr, S.; Nguyen, T.; Mahmoud, E.; Schopf, E.; Fomina, N.; Almutairi, A. Biocompatible polymeric nanoparticles degrade and release cargo in response to biologically relevant levels of hydrogen peroxide. *J. Am. Chem. Soc.* **2012**, *134*, 15758–15764. [CrossRef] [PubMed]
38. Rehor, A.; Hubbell, J.A.; Tirelli, N. Oxidation-sensitive polymeric nanoparticles. *Langmuir* **2005**, *21*, 411–417. [CrossRef] [PubMed]
39. Broaders, K.E.; Grandhe, S.; Fréchet, J.M. A biocompatible oxidation-triggered carrier polymer with potential in therapeutics. *J. Am. Chem. Soc.* **2011**, *133*, 756–758. [CrossRef] [PubMed]
40. Yoshida, K.; Awaji, K.; Shimizu, S.; Iwasaki, M.; Oide, Y.; Ito, M.; Dairaku, T.; Ono, T.; Kashiwagi, Y.; Sato, K. Preparation of microparticles capable of glucose-induced insulin release under physiological conditions. *Polymers* **2018**, *10*, 1164. [CrossRef]
41. Inoue, H.; Anzai, J. Stimuli-sensitive thin films prepared by a layer-by-layer deposition of 2-iminobiotin-labeled poly(ethyleneimine) and avidin. *Langmuir* **2005**, *21*, 8354–8359. [CrossRef] [PubMed]
42. Pasternack, R.F.; Goldsmith, J.I.; Szép, S.; Gibbs, E.J. A spectroscopic and thermodynamic study of porphyrin/DNA supramolecular assemblies. *Biophys. J.* **1998**, *75*, 1024–1031. [CrossRef]
43. Suenaga, H.; Nango, M.; Sugiyama, T.; Iwasaki, T.; Takeuti, Y.; Shinkai, S. DNA cleavage by a polyethylenimine-appended porphyrin. *Chem. Lett.* **2000**, *29*, 306–307. [CrossRef]
44. Sato, K.; Takahashi, M.; Ito, M.; Abe, E.; Anzai, J. H_2O_2-induced decomposition of layer-by-layer films consisting of phenylboronic acid-bearing poly(allylamine) and poly(vinyl alcohol). *Langmuir* **2014**, *30*, 9247–9250. [CrossRef] [PubMed]
45. Sato, K.; Awaji, K.; Ito, M.; Anzai, J. Preparation of H_2O_2-induced poly(amidoamine) dendrimer release nanofilms. *Colloid Polym. Sci.* **2017**, *295*, 877–882. [CrossRef]
46. Sato, K.; Takahashi, M.; Ito, M.; Abe, E.; Anzai, J. Glucose-induced decomposition of layer-by-layer films composed of phenylboronic acid-bearing poly(allylamine) and poly(vinyl alcohol) under physiological conditions. *J. Mater. Chem. B* **2015**, *3*, 7796–7802. [CrossRef]
47. Sato, K.; Shimizu, S.; Awaji, K.; Hitomi, O.; Anzai, J. Lactate-induced decomposition of layer-by-layer films composed of phenylboronic acid-modified poly(allylamine) and poly(vinyl alcohol) under extracellular tumor conditions. *J. Colloid Interface Sci.* **2018**, *510*, 302–307. [CrossRef] [PubMed]